Citation: Proceedings of SPIE, Vol: 9510, pp. 951001 - 951012 (2015)

https://doi.org/10.1117/12.2179446

# Polarizers for a spectral range centered at 121.6 nm operating by reflectance or by transmittance

Juan I. Larruquert[1*], A. Marco Malvezzi[2], Angelo Giglia[3], José A. Aznárez[1], Luis Rodríguez-de Marcos[1], José A. Méndez[1], Paolo Miotti[4], Fabio Frassetto[4], Giuseppe Massone[5], Gerardo Capobianco[5], Silvano Fineschi[5], Stefano Nannarone[3]

[1]GOLD, Instituto de Óptica-Consejo Superior de Investigaciones Científicas, Madrid, Spain
[2]Universitá di Pavia, Pavia, Italy
[3]Istituto Officina dei Materiali -Consiglio Nazionale delle Ricerche, Trieste, Italy
[4]Institute of Photonics and Nanotechnologies-National Council for Research, Padua, Italy
[5]INAF - Osservatorio Astrofisico di Torino, Torino, Italy

## ABSTRACT

Polarimetry is a powerful tool to interpret how the coronal plasma is involved in the energy transfer processes from the Sun's inner parts to the outer space. Space polarimetry in the far ultraviolet (FUV) provides essential information of processes governed by the Doppler and Hanle resonant electron scattering effects. Among the key FUV spectral lines to observe these processes, H I Lyman α (121.6 nm) is the most intense. Some developing or proposed solar physics missions, such as CLASP, SolmeX, and COMPASS, plan to perform polarimetry at 121.6 nm. Classical solutions, such as a parallel plate of a transparent material, either $MgF_2$ or LiF, result in a modest efficiency of the passing polarization component. The development of more efficient linear polarizers at this wavelength will benefit future space instruments.

A research has been conducted to develop polarizers based on $(Al/MgF_2)_n$ multilayer coatings in a band containing 121.6 nm, to obtain a significant efficiency increase over plates. Coatings operating by reflectance resulted in a high efficiency after approximately one year of storage under nitrogen. In parallel, coating polarizers operating by transmittance have been prepared for the first time. Transmissive polarizers have the advantage that they involve no deviation of the beam. As a further benefit, the developed transmittance polarizers additionally incorporate filtering properties to help reject wavelengths both shortwards and longwards of a band containing 121.6 nm. Hence a polarizer combined with a filter is obtained with a single device. The combined polarizer-filter could enable a higher performance polarimeter for solar physics if the use of a separate filter to isolate Lyman α turns unnecessary.

**Keywords:** polarizers, multilayer coatings, far ultraviolet, vacuum ultraviolet, polarimetry, solar corona, Hanle effect

## 1. INTRODUCTION

The magnetic field plays a crucial role in the dynamics of the solar chromosphere and corona. Hence, measuring the magnetic field in the solar corona is crucial to understanding and predicting the Sun's generation of space weather that affects communications, space flight, and power transmission. Because the changing coronal magnetic field drives the processes at the origin of space weather, the ability to measure the field changes will enable us to understand the basic underlying physics and predict space weather events.

In the high-temperature ($10^4$ – $10^6$ K) chromosphere and corona, strong resonance lines are formed in the ultraviolet. Some anisotropic radiation pumping processes induce atomic polarization in the energy levels involved in the transition of the emitted radiation. The most interesting wavelength range for the diagnostics of solar and stellar magnetic fields via spectral-line-polarimetry of the Zeeman and Hanle effects is the 90-150 nm interval in the far ultraviolet (FUV). In this spectral range many hydrogen-like emission lines are formed in the hot ($10^4$-$10^7$ K) astrophysical plasmas, in particular the neutral hydrogen (HI) Lyman-series lines and the O VI and C IV lines. Among the brightest lines sensitive to the

* larruquert@io.cfmac.csic.es; phone: 34- 915618806 ext 330; fax: 34-914117651

Hanle effect is the H I Lyman-α line at 121.6 nm [1,2,3,4,5,6]. It was shown [2,7] that a degree of polarization of up to 20% can be expected in the H I Lyman-α line in the solar corona. Using the SOHO/SUMER spectrograph, Raouafi et al.[8,9] achieved the first detection of the Hanle polarization signal in the corona using the O VI doublet at 103.2/103.8 nm. These pioneering results were obtained with an instrument that was not designed to measure polarization and they established without any ambiguity that a dedicated instrument will be able to provide routine global coronal magnetic field diagnostics.

Future instruments for polarimetric observations of the chromosphere and the solar corona will require more efficient linear polarizers at H Lyman α at 121.6 nm. Linear polarizers operating at short wavelengths are also needed for an always increasing number of applications, including imaging instrumentation for astrophysics, synchrotron radiation, ellipsometry, lasers, atomic and molecular physics, solid state physics, particle-matter interaction, magnetic and chiral-material analysis, etc.

The simplest polarizers at 121.6 nm and at most of the FUV are crystal plates of transparent fluorides working in reflection at an angle close to Brewster angle, which gives $R_p \approx 0$ (p or TM component). A limitation of these elements is their modest reflectance at the non-extinguished component $R_s$ (s or TE component), which results in a moderate polarizer efficiency. Plates must be made of basically transparent materials, most often LiF and $MgF_2$ [10,11,12,13,14]. Even though polarizers at Brewster angle are good at rejecting one polarization component when they operate by reflection, this property has been often used in the reverse way, i.e., by transmission, due to the benefit of not bending the optical axis. In transmission, since the $T_p/T_s$ ratio is not large, a series of inclined plates can be used to enhance this number; the drawback of this is that the combined transmittance at the passing polarization component ($T_p$) is usually small. Hence, a pile of plates of LiF [15,16,17,18] in transmission mode has been most often used; plates of $MgF_2$ have been also used, in spite of its residual birefringence [19].

Efficient polarizers can be developed with the use of multilayer coatings. The benefit of coatings versus transparent plates is the degrees of freedom in the coating design that are used to increase performance above the modest value that can be obtained with the plate (or pile-of-plates) at Brewster angle. In the range of interest in this research, reflective coating polarizers have been prepared with $Al/MgF_2$ multilayers among a few other coatings. Hass and Hunter [13] developed a 3-mirror polarizer, with the benefit of no deviation of the incoming beam; it combined two $Al/MgF_2$ mirrors and a $MgF_2$ plate working close to Brewster angle; it had a good $R_s/R_p$ efficiency ratio in a wide spectral range including the FUV and shortwards, but it had a modest efficiency for the non-extinguished component of ~17% close to 121.6 nm. Kim et al. [20] designed a polarizer for 121.6 nm based on a 3-layer $MgF_2/Al/MgF_2$ coating deposited on an Al substrate. Bridou et al. [21] reported on efficient polarizers at 121.6 nm based on various of coatings, including a $(Al/MgF_2)_2$ four layer coating on glass. Kano et al. [22] fabricated a polarizer based on the $(Al/MgF_2)_2$ polarizer design of Ref. 21, and obtained a good efficiency at 121.6 nm. Other coatings have been used to make polarizers, both by reflection at a single mirror [23,24,25] and also at a 3-mirror [26,27,28,29,30,31] or 4-mirror [32] configuration to keep the optical axis unmoved, although the latter configurations result in low-efficiency polarizers that besides may be difficult to align. More extensive information on polarizers for the FUV can be found in various reviews [33,34,35].

In a recent paper, transmissive polarizers in this same range based on coatings have been developed for the first time [36]. In this research, the same group has attempted new designs of transmissive polarizers based on $Al/MgF_2$ multilayer coatings that cover a certain spectral range around 121.6 nm. We present the new transmissive polarizers. Section 2 describes the experimental techniques employed in this research for coating preparation and polarization measurements. Section 3 presents the designs and the FUV transmittance measurements for the two polarization components on various coatings as a function of wavelength and incidence angle, along with a summary of previous results on reflective and transmissive polarizers.

## 2. EXPERIMENTAL TECHNIQUES

### 2.1 Sample preparation

Coating polarizers operating both by reflection and by transmission were designed and prepared at GOLD. $(Al/MgF_2)_n$ multilayer coatings (Al is always the first layer and $MgF_2$ the last one) were deposited in a high-vacuum chamber pumped with a turbomolecular system and a liquid-$N_2$ cooled, Ti sublimation pump. Both Al and $MgF_2$ films were deposited by evaporation using W boats ($MgF_2$) and filaments (Al). 99.999% pure Al and VUV-grade $MgF_2$ were used as evaporant materials. The base pressure in the chamber was $10^{-5}$ Pa.; pressure increased during deposition to ~$10^{-4}$ Pa (Al) and ~$5\times10^{-5}$ Pa ($MgF_2$). Substrates were pieces of polished float glass (reflective polarizers) or $MgF_2$ crystals cut perpendicular to the c-axis (transmissive polarizers), which were not intentionally heated or cooled during or after deposition. The distance between the evaporation source and the substrate was 30 cm. Film thickness was measured with a quartz-crystal monitor, that had been calibrated through Tolansky interferometry, i.e., through multiple-beam interference fringes in a wedge between two highly reflective surfaces. Before the initial measurements, samples were kept in residual vacuum most of the time after preparation, and the approximate time of exposure to the atmosphere is specified for each sample. For samples prepared for previous campaigns in the synchrotron, after the initial measurements were completed, samples were stored in a box filled with nitrogen until they were taken out to measure them again.

### 2.2 Experimental setup for reflectance and transmission measurements

The polarization characteristics of the coatings were measured at the BEAR (Bending magnet for Emission, Absorption and Reflectivity) beamline at ELETTRA synchrotron (Trieste, Italy). BEAR is an apparatus intended for optical spectroscopic study of anisotropic systems [37], of the interfaces of multilayer systems [38,39,40] and particularly suitable for characterization of polarizers [36,41].

Specular reflectance and transmission measurements of polarizers in s (TE) and p (TM) polarization incidence ($R_s$ and $R_{p,}$ and $T_s$ and $T_{p,}$, respectively), were performed between 6 eV (207 nm) and 11 eV (112.7 nm) with linearly polarized light [degree of linear polarization $((I_s-I_p)/(I_s+I_p)=0.99$]. The angles of incidence for reflected or transmitted light were set with an accuracy of ~ (1/10)° for both reflection and transmission measurements. The degree of polarization of light, propagating along the *x* axis, was set by a variable aperture slit (see BEAR web [42]) accepting light of the bending magnet emission in an angle range within ±0.17 mrad with respect to the synchrotron orbit plane. The cross section of the monochromatic light spot at the focus position was set at 400x400 $\mu m^2$ horizontal x vertical, with a divergence of ~ 20 mrad**,** with an energy band width of ~60 *meV* ( $\Delta E/E=10^{-2}$) and with the incident electric field contained in the *yz* plane. The incident flux was ~ $10^9$ photons/s. Higher order rejection was accomplished by an optical grade thick LiF crystal (Crystec) filter. The light polarization at the sample site was measured by using two alternate methods. In one case a single analyzer element – in the present case, a LiF crystal slab mounted at the Brewster angle of the energy range at issue– was rotated together with the light detector mounted on the specular direction as a rigid assembly around the impinging light *x* axis (see for instance Ref. [43]). In the other case $R_s$ and $R_{p,}$ were measured with the LiF slab mounted at the Brewster angle and the major and minor axes of polarization of the ellipses were retrieved (within the usual approximations). In the s incidence the sample normal was contained in the *xz* plane. Conversely, the normal was contained in the *xy* plane in p incidence. The detector and sample assembly rotated rigidly around the *x* axis in order to accomplish the two polarization incidence geometries without changing the relative sample-detector position. A silicon diode (IRD-AXUV100) was used as light detector. Measurements were taken in DC current by a picoammeter. The impinging flux was monitored by measuring with a picoammeter the refocusing mirror drain current.

Transmission and reflectivity data were obtained by averaging at each energy a set of light and dark (eventually subtracted) measurements. The overall accuracy of this method resulted in a statistical error σ of the single measurement ~$10^{-13}$ A resulting in a lowest measurable flux (both in transmission and reflection) ~ $10^6$ photons/s with a detection dynamics of three orders of magnitude. For both transmittance and reflectance measurements, the beam impinged on the sample from the coating side.

## 3. RESULTS AND DISCUSSION

### 1. Reflective polarizers

The present research started with reflective polarizers for 121.6 nm based on $Al/MgF_2$ multilayer coatings. The previous research by Bridou et al. [21] used $(Al/MgF_2)_2$ multilayers (i.e., two bilayers) and measurements were performed at the target wavelength of 121.6 nm. Our designs of polarizers attempted to get the largest efficiency in the broadest possible spectral range including 121.6 nm. This led us to design multilayers with increased degrees of freedom, i.e., the number of layers with their thicknesses to be optimized. Hence the number of bilayers was increased to three and even four in order to obtain polarizers with a larger spectral range of operation.

The performance of two reflective polarizers prepared in this research is presented below. Both samples were designed with three bilayers; each design was optimized at a specific incidence angle. In a previous publication [44]. contour plots of both $R_{par}$ and $R_{per}$ ($R_{par}$ and $R_{per}$ are the reflectance measured in a plane that is parallel and perpendicular, respectively, to the storage ring) as a function of wavelength and angle of incidence were displayed for one polarizer, which showed that the polarizer could be used at any wavelength between ~113 and 134 nm by selecting the optimum incidence angle.

In ideal conditions, $R_{par}$ and $R_{per}$ would be equivalent to $R_p$ and $R_s$, respectively. In practice, full light polarization is only available in the exact storage ring plane; however, in order to have a sufficient number of photons, a beam with some extension in the direction perpendicular to the storage ring must be used for measurements, which results in a beam with some residual elliptical polarization. The degree of polarization of the incoming beam, as it leaves the ring, may be slightly modified by the beamline optics and by some slight deviation of the measurement planes with respect to the storage ring plane (or its perpendicular). Hence the present $R_{par}$ and $R_{per}$ measurements are expected to be a higher and a lower limit, respectively, of the real $R_p$ and $R_s$, or in other words, real $R_s$ and mainly $R_p$ are expected to give an even better performance than what is plotted in the below figures. An analogous situation occurs with $T_{par}$-$T_{per}$ and $T_s$-$T_p$ for transmissive polarizers in the next subsection. A comprehensive description of the polarization of synchrotron radiation can be found in the literature [45].

Figs. 1 and 2 display $R_{par}$ and $R_{per}$ measured for two samples after several months of storage in nitrogen. For the sample plotted in Fig. 1, $R_{par}$ was slightly less than 0.01 at 121.6 nm for 60° and 65°, with a value of $R_{per}$ as large as 0.69 at 65°; best performance was obtained at 65° in the range of ~120.8-128 nm. For the sample plotted in Fig. 2, $R_{par}$=0.017 and $R_{per}$=0.725 were measured at 70°; with a value of $R_{par}$ below 0.02 at some incidence angle in the 117.5-125.6-nm spectral range; corresponding $R_{per}$ stood at 0.70 and above.

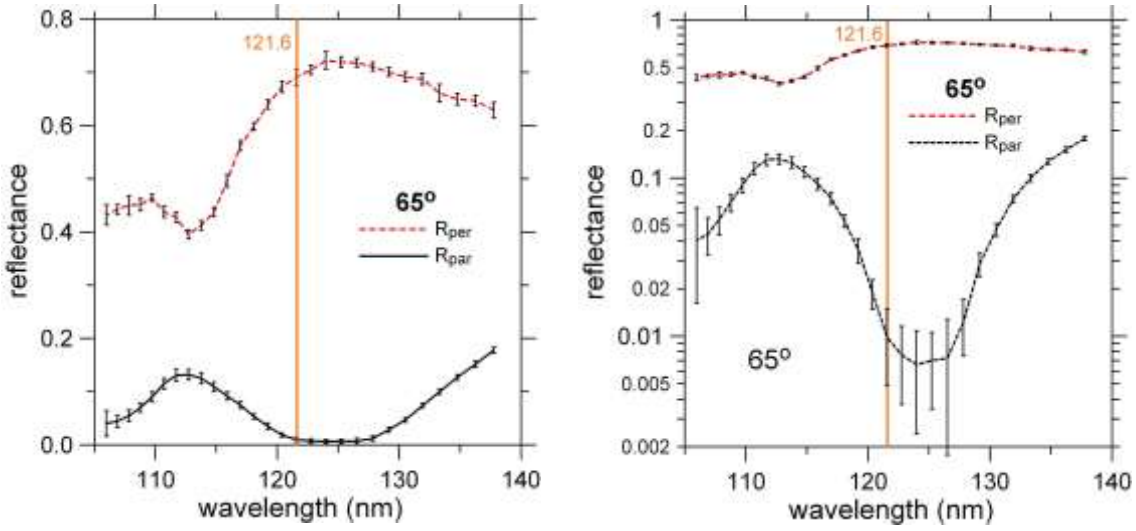


Fig. 1. Linear (left) and log-axis (right) plot of $R_{par}$ and $R_{per}$ versus wavelength for a sample aged of 8 months in nitrogen (plus seven weeks in residual vacuum) at 65° from the normal

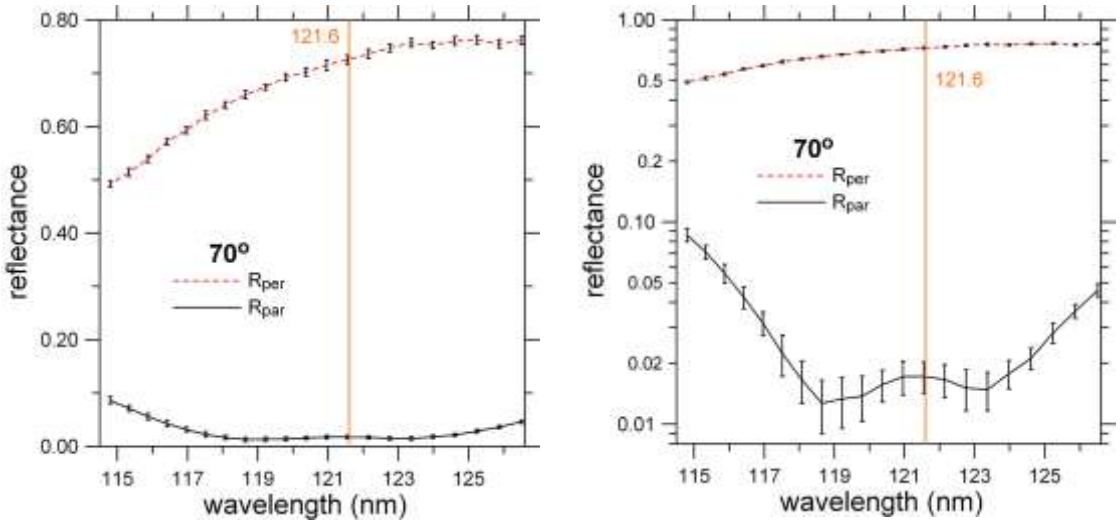


Fig. 2. Linear (left) and log-axis (right) plot of $R_{par}$ and $R_{per}$ versus wavelength for a sample aged of 13 months in nitrogen (plus seven weeks in residual vacuum) at 70° from the normal

The above aged samples, consisting of $(Al/MgF_2)_3$ coatings, result in a somewhat better performance at 121.6 nm than coatings based on the design $(Al/MgF_2)_2$ [21]; compared with the coatings with two bilayers, sample in Fig. 1 has a lower $R_p$ with the same $R_s$, whereas sample in Fig. 2 has a larger $R_s$, while $R_p$ is in the short edge of the reported range of values. The present values are for aged samples whereas information on polarizer ageing was not given in Ref [21]. Additionally, polarizing properties were found in our research in a spectral range that extends both below and above 121.6 nm.

**2. Transmissive polarizers**

Polarizers in a range around 121.6 nm operating by transmittance have been recently developed [36]. The idea to develop such a polarizer was to avoid the beam deviation (except for a minor lateral shift) entered by a reflectance polarizer; this property of transmissive polarizers can simplify the geometry of an instrument. The design of transmissive polarizers is given in Table 1.

Table 1. Optimization angle (from the normal) and optical layer thicknesses (in quarterwaves) of transmissive polarizer multilayer coatings; 1: innermost bilayer; 3: outermost bilayer

| Sample | Opt. angle | Optical layer thickness (quarterwaves) | | | | | |
|---|---|---|---|---|---|---|---|
| | | Al 1 | $MgF_2$ 1 | Al 2 | $MgF_2$ 2 | Al 3 | $MgF_2$ 3 |
| T1 | 78° | 0.002 | 0.13 | 0.003 | 0.11 | 0.003 | 0.32 |
| T2 | 75° | 0.004 | 0.16 | 0.005 | 0.15 | 0.004 | 0.39 |
| T3 | 70° | 0.005 | 0.22 | 0.007 | 0.21 | 0.005 | 0.52 |
| T4 | 75° | 0.004 | 0.15 | 0.005 | 0.14 | 0.004 | 0.38 |

Fig. 3 displays $T_{per}$ and $T_{par}$ measured for the first developed transmittance polarizer T1 after 13 months of storage in nitrogen. Measurements were performed as a function of wavelength at 73° and at 78°. With transmissive polarizers, the role played by the two polarization components is inverted compared to reflective polarizers: now the perpendicular component is more suitable to be minimized. At 121.6 nm, $T_{per}$ and $T_{par}$ were in the range of 0.005-0.008 and 0.096-0.11, respectively. Maximum polarization efficiency is obtained in the ~124-129-nm range. Some shift of the polarization

range is observed between the two measured incidence angles; an advantage of a transmissive polarizer is that it can be somewhat tuned in wavelength by rotation**,** with no essential beam shift and no deviation.

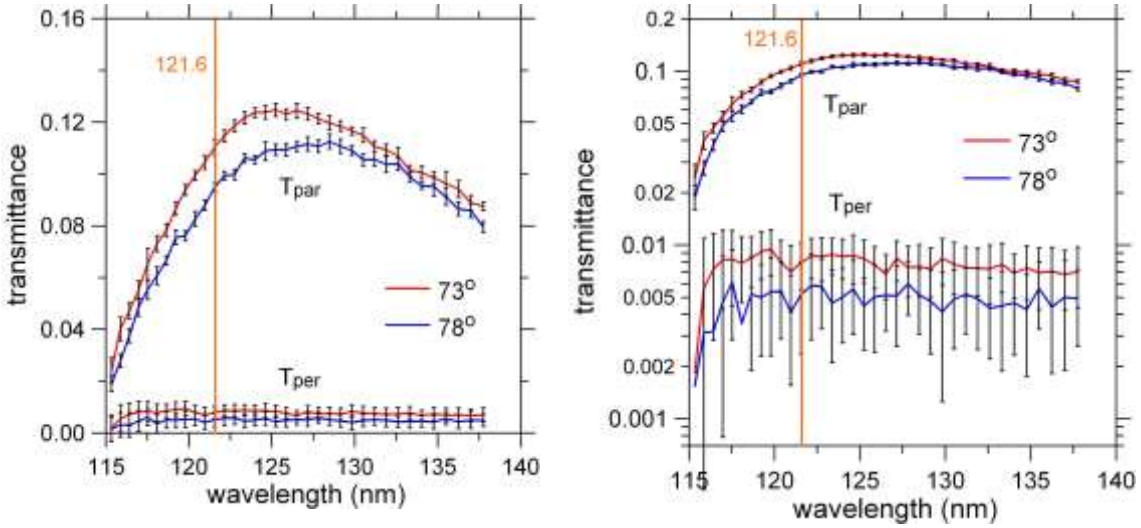


Fig. 3. Linear (left) and log-axis (right) plot of $T_{per}$ and $T_{par}$ versus wavelength for sample T1 aged of 13 months in nitrogen (plus two weeks in residual vacuum) for two angles of incidence (measured from the normal)

For transmittance polarizers we used $MgF_2$ substrates so that the beam impinged from the coating side. Hence, the retardation due to $MgF_2$ birefringence is introduced after the beam has crossed the coating, so that it does not result in an intensity change on the detector. To use the polarizer in a polarimeter, a LiF substrate could be used for its lack of birefringence; a $MgF_2$ substrate could be also used if cut with the optics axis along the beam propagation direction in the material.

The transmissive polarizer plotted in Fig. 3 displays filtering properties, with a peak transmittance wavelength not far from 121.6 nm (in the ~125-128-nm range). In that first design, the filtering was obtained by serendipity**,** since no requirement for filtering was included in the design. In fact, no measurement was performed outside the displayed data but calculations predict a 121.6-to-200 nm transmittance ratio of ~7.

In the following filter campaign, we have prepared new transmittance polarizers in whose design, the requirement of filtering the long FUV (at ~200 nm) has been added in the design minimization function. Three such polarizers T2, T3, and T4 with slight design differences were prepared. Fig. 4 displays the transmittance of T2 through T4.

Measurements on samples T2, T3, and T4 were performed on samples only exposed to normal air for about seven, two, and two days, respectively, plus a storage period in vacuum of one to two weeks. For samples T2, T3, and T4 measurements were extended up to 205 nm in order to check their capacity to reject the long FUV. This extension increased the time necessary to characterize each sample, which resulted in shorter time devoted to measurements at each wavelength and hence to a larger uncertainty, particularly for measurements with low transmittance (i.e., $T_{per}$ in the whole range and $T_{par}$ in the long-wavelength range). To somewhat reduce measurement oscillations for $T_{per}$ for wavelengths shorter than 160 nm, we averaged each measurement with the measurements at the next longer and shorter wavelength, and these averages are plotted in Fig. 4; measurements for wavelengths shorter than 130.5 nm, i.e., for energies larger than 9.5 eV, were performed every 0.05 eV (every 0.25 eV below 9.5 eV). Above 160 nm, data plotted in Fig. 4 correspond to the average of $T_{par}$ and $T_{per}$, i.e., $T_{aver}=0.5*(T_{par}+T_{per})$, which assumes that long-wavelength FUV light impinging on the solar-physics polarimeter is basically nonpolarized. The best sample at 121.6 nm was T4 at 70°, with $T_{par}\approx10\%$, $T_{per}\approx0.3\%$, and with a transmittance in the long FUV of ~0.6%. This gives a filter performance, defined as $T_{par}$(121.6 nm)/$T_{aver}$(long FUV), of ~16. As a reminder, previously developed transmittance filter (T1) was estimated to have a ratio of ~7 for values of $T_{par}$ and $T_{per}$ at 121.6 nm similar to T4, so that the objective of increasing long-FUV rejection has been accomplished. Anyway, some decrease of $T_{par}$ at the peak wavelength range can be expected for the present samples after a longer ageing period. The mentioned ratio of 16 starts to be comparable to what can be obtained with available transmittance filters tuned at 121.6 nm, which typically operate at normal incidence. The present polarizers are expected to reject radiation even better beyond 200 nm up to the visible and infrared, due to the Al content

in the multilayer. All four polarizers have their $T_{par}$ peak at ~125 nm, rather than at 121.6 nm, which is attributed to the increasing transparency of $MgF_2$ films longwards of 121.6 nm.

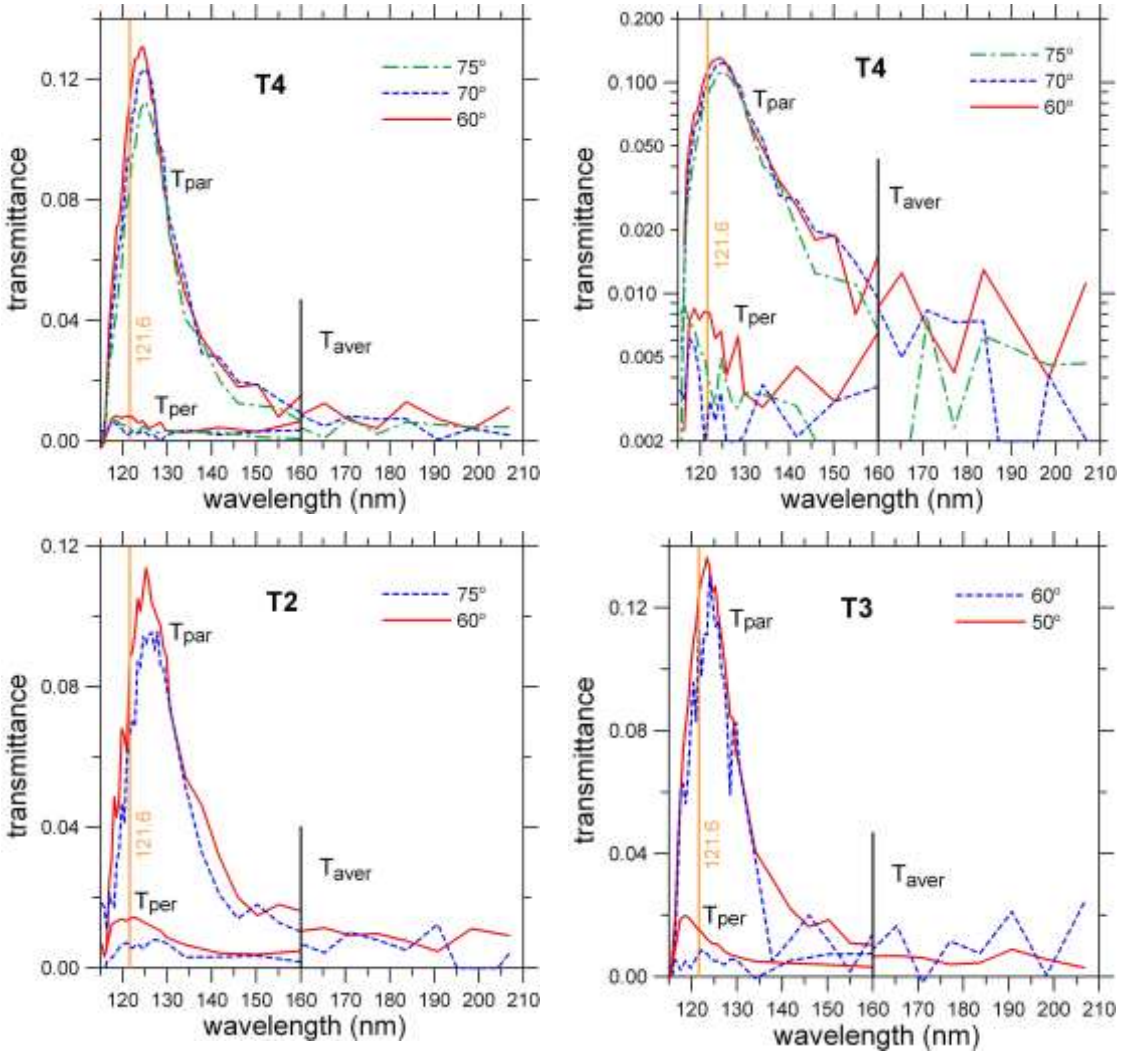


Fig. 4. Linear (top left) and log-axis (top right) plot of $T_{per}$ and $T_{par}$ versus wavelength for sample T4 for three angles of incidence. Linear plot of $T_{per}$ and $T_{par}$ versus wavelength for sample T2 (bottom left) and T3 (bottom right) for two angles of incidence. Samples were exposed to the atmosphere for two to seven days (plus one to two weeks in residual vacuum). Angles are measured from the normal

The measured filtering properties of transmissive polarizers may result in that a polarimeter operating at 121.6 nm, such as for space observation of the solar corona and chromosphere, may use a single device for both linear polarizing and out-of-band rejection, with an improved efficiency for not requiring an extra filter. The use of transmissive instead of reflective polarizers also simplifies the polarimeter geometry.

Samples T2 and T3 are somewhat inferior to T4. Compared to T4, sample T3 at 50° displays a little larger $T_{par}$ at 121.6 nm, with similar long-wavelength rejection, but with larger $T_{per}$.

We evaluate the efficiency of a polarizer in providing linearly polarized light in terms of the modulation factor:

$$\mu = \frac{T_p - T_s}{T_p + T_s} \tag{1}$$

In an ideal polarizer, μ approaches 1 and simultaneously $T_p$ is large. A useful parameter encompassing these two quantities is called the figure of merit κ, which is defined as [46]:

$$\kappa = \mu\sqrt{T_{aver}} \tag{2}$$

where T is the transmittance averaged over the two polarizations: $T_{aver}=(T_s+T_p)/2$, which will be referred to as throughput. κ provides information on the trade-off between polarization efficiency and throughput. We want κ to be as large as possible, keeping in mind that the maximum possible κ value (for a perfect polarizer) is $1/2^{0.5}= 0.71$.

Figs. 5 through 8 display μ and κ versus wavelength for the transmissive polarizers T1 through T4, where $T_s$ and $T_p$ of Eq. (1) were replaced with $T_{per}$ and $T_{par}$, respectively; as a reminder T1 was measured after a long storage time in nitrogen, whereas T2 through T4 were measured after a short contact with the atmosphere. Using μ as an evaluation parameter, the best transmissive polarizer at 121.6 nm is T4 at 70°, with μ=0.95. Using κ as the evaluation parameter, best samples are T4 at 70° with and T1 at 73° with κ=0.21, although measurements for T4 were taken for a fresh sample and these numbers can somewhat decrease over time. If such a decrease were negligible, present sample T4 would provide an enhanced efficiency μ with a similar throughput κ compared to the original transmissive polarizer T1, with the addition of an increased long-wavelength rejection. For sample T1, μ and κ versus wavelength present a relatively flat shape, whereas for samples T2 through T4, κ presents a faster decrease above 126 nm, which is attributed to the added requirement of long-wavelength rejection for the latter samples.

Let us compare the present results with the performance reported in the literature. Walker [15] used sets of four or six LiF piles of plates; his measurements result in μ=0.82, κ=0.17 (6 plates), and μ=0.68, κ=.23 (4 plates). Compared to the present results for T4 and 70º, the coating polarizer is superior to the 6-plate system both on μ and κ, and it is also far superior to the 4-plate system in μ, although it is slightly inferior to the 4-plate system in κ. But the good numbers of the coating polarizer combine with its rejection capacity of the long wavelengths.

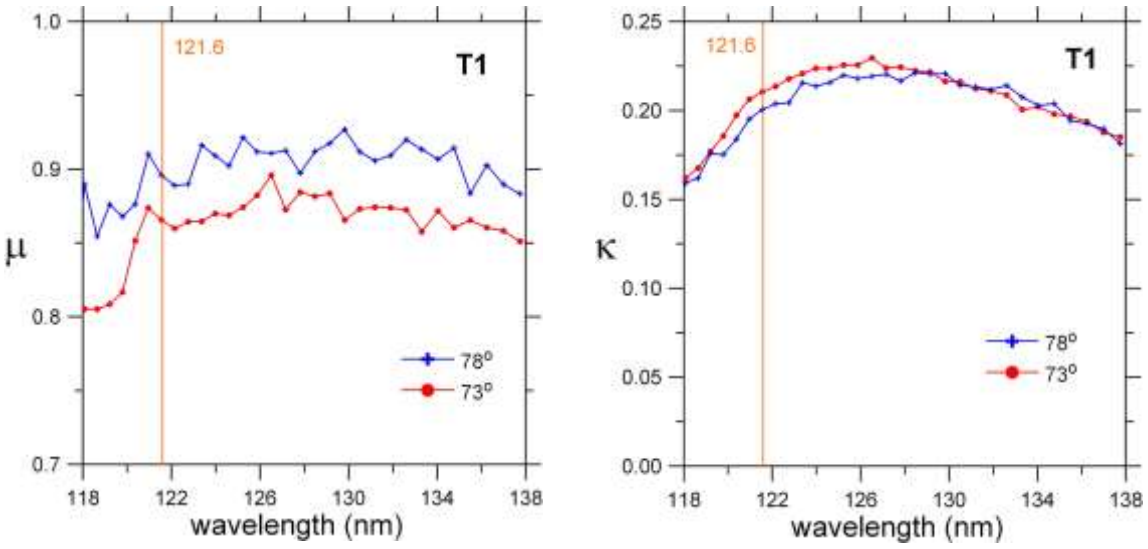


Fig. 5. μ (left) and κ (right) versus wavelength for aged T1 sample

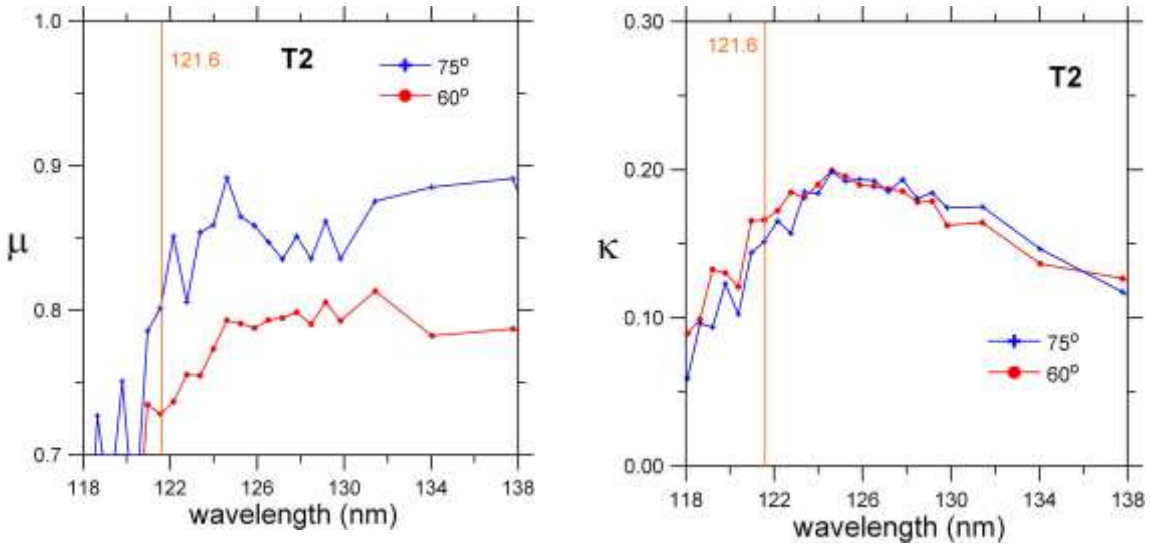


Fig. 6. μ (left) and κ (right) versus wavelength for fresh T2 sample

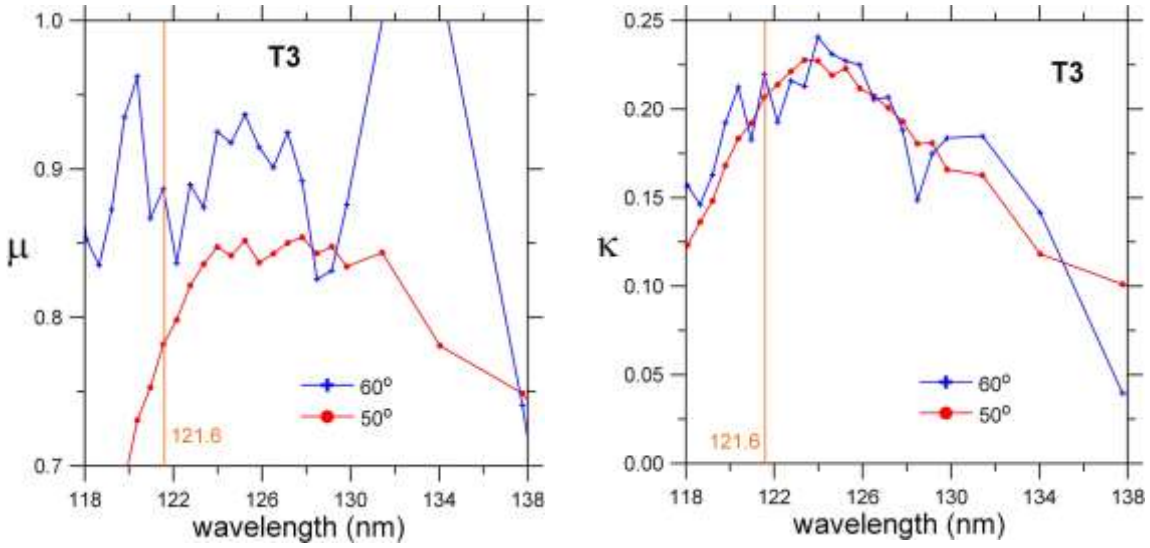


Fig. 7. μ (left) and κ (right) versus wavelength for fresh T3 sample

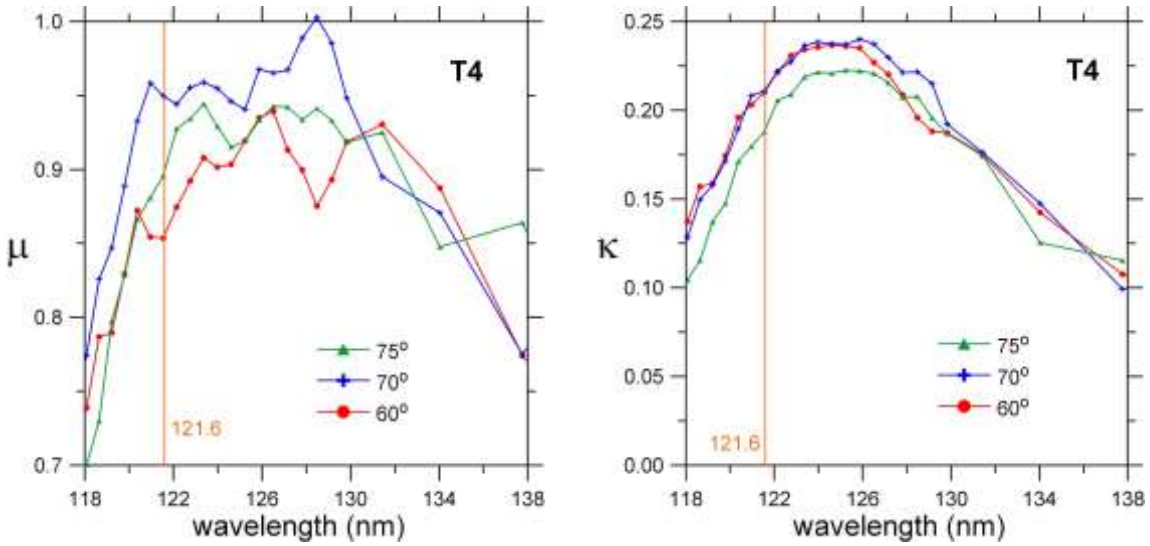


Fig. 8. μ (left) and κ (right) versus wavelength for fresh T4 sample

## SUMMARY AND CONCLUSIONS

Efficient linear polarizers at 121.6 nm based on ($Al/MgF_2$) multilayer coatings have been designed, prepared, and their efficiency measured in two perpendicular planes of incidence. Polarizers operating by either reflectance or transmittance have been developed. A summary of a previous research on reflective polarizers has been given, where polarizers with 3 or 4 bilayer coatings are more efficient than previously deposited polarizers with 2 bilayer coatings. Furthermore, a research to develop transmittance polarizers has been conducted because of their advantage of inducing no light-beam deviation. A previously developed polarizer operating by transmittance showed that it simultaneously involved some filtering properties. New transmissive polarizers have been developed with the added requirement of a high rejection of the out-of-band. Best result are obtained for a shortly aged transmissive polarizer operating at 70°, with the following parameters: $T_p(121.6)\approx 10\%$, $T_s(121.6)\approx 0.3\%$, and a $T_p(121.6\text{ nm})/T_{aver}$(long FUV) ratio of ~16. The figure of merit of the coating polarizer ($\kappa=0.21$) is very similar to what can be obtained with a polarizer based on a pile of plates ($\kappa\leq 0.23$), but the former operates also as a bandpass filter. The measured filtering properties of transmissive polarizers may result in that a polarimeter operating at 121.6 nm, such as for space observation of the solar corona and chromosphere, may use a single device for both linear polarizing and out-of-band rejection, with an improved efficiency for not requiring an extra filter; the use of transmissive instead of reflective polarizers also simplifies the polarimeter geometry.

## ACKNOWLEDGMENTS

We acknowledge support by the European Community–Research Infrastructure Action under the FP6 ‘Structuring the European Research Area’ Programme (through the Integrated Infrastructure Initiative ‘Integrating Activity on Synchrotron and Free Electron Laser Science’); measurements were performed under ELETTRA proposal numbers 20115134, 20120059, 20125119, 20130201, 20135237, and 20140171. This work was also supported by the National Programme for Research, Subdirección General de Proyectos de Investigación, Ministerio de Ciencia e Innovación, project numbers AYA2010-22032 and AYA2013-42590-P. We also acknowledge support by the Italian Ministry of University and Research (MIUR) under the Programmi di Ricerca Scientifica di Rilevante Interesse Nazionale—Bando 2012.

## REFERENCES

[1] Sahal-Bréchot, S., “Role of collisions in the polarization degree of the forbidden emission lines of the Solar Corona. II - Depolarization by electron impact and calculation of the polarization degree of the Green line of Fe XIV,” Astron. Astrophys. **36**, 355 (1974).

[2] Bommier, V., and Sahal-Bréchot, S., "The Hanle effect of the coronal Lα line of hydrogen: Theoretical investigation," Sol. Phys. **78**, 157-178 (1982).
[3] Fineschi, S., "Space-based Instrumentation for Magnetic Field Studies of Solar and Stellar Atmospheres," ASP Conf. Ser. **248**, 597-605 (2001).
[4] Bommier, V., "Hanle effect from a dipolar magnetic structure: the case of the solar corona and the case of a star," Astron. Astrophys. **539**, A122 (2012).
[5] Fineschi, S., Hoover, R. B., and Walker II, A. B. C., "Hydrogen Lyman α coronagraph/polarimeter," Proc. SPIE **1546**, 402-413 (1991).
[6] Fineschi, S., Hoover, R. B., Zukic, M., Kim, J., Walker II, A. B. C., and Baker, P. C., "Polarimetry of the HI Lyman α for coronal magnetic field diagnostics," Proc. SPIE **1742**, 423-438 (1992).
[7] Fineschi, S., Hoover, R. B., Fontenla, J. M., and Walker II, A. B. C., " Polarimetry of extreme ultraviolet lines in solar astronomy," Opt. Eng. **30**, 1161-1168 (1991).
[8] Raouafi, N.-E., Lemaire, P., and Sahal-Bréchot, S., "Detection of the O VI 103.2 nm line polarization by the SUMER spectrometer on the SOHO spacecraft," Astron. Astrophys. **345**, 999-1005 (1999).
[9] Raouafi, N.-E., Harvey, J. W., and Solanki, S. K., "Properties of solar polar coronal plumes constrained by ultraviolet coronagraph spectrometer data," Astrophys. J. **658**, 643-656 (2007).
[10] Metcalf, H., Baird, J. C., "Circular polarization of vacuum ultraviolet light by piezobirefringence" Appl. Opt. **5**, 1407-1410 (1966).
[11] Ott, W. R., Kauppila, W. E., and Fite, W. L., "Polarization of Lyman-Alpha radiation produced in collisions of electrons and hydrogen atoms," Phys. Rev. Lett. **19**, 1361-1363 (1967).
[12] Teubner, J. O., Kauppila, W. E., Fite, W. I., Girnius, R. J., "Polarization of Lyman-α radiation produced in charge-transfer collisions between protons and the inert gases," Phys. Rev. A **2**, 1763-1767 (1970).
[13] Hass, G., Hunter, W. R., "Reflection polarizers for the vacuum ultraviolet using Al + MgF2 mirrors and an MgF2 plate," Appl. Opt. **17**, 76-82 (1978).
[14] Hippler, R., Faust, M., Wolf, R., Kleinpoppen, H., and Lutz, H. O., "Polarization studies of H(2p) charge-exchange excitation: $H^+$-Ar collisions," Phys. Rev. A **31**, 1399-1404 (1985).
[15] Walker, W. C., "Pile-of-Plates Polarizer for the Vacuum Ultraviolet," Appl. Opt. **3**, 1457-1460 (1964).
[16] Hinson, D. C., "State of polarization of light from a normal-incidence vacuum-ultraviolet monochromator," J. Opt. Soc. Am. **56**, 408 (1966).
[17] Heath, D. F., "A far ultraviolet polarization analyzer for rocket use" Appl. Opt. **7**, 455-460 (1968).
[18] Keim, M. , Werner, A., Hasselkamp, D., Schartner, D.-H., Lüdde, H. J., Achenbach, A., and Kirchner, T., "Lyman-α line polarization after proton impact on atomic hydrogen," J. Phys. B: At. Mol. Opt. Phys. **38**, 4045–4055 (2005).
[19] Winter, H., and Ortjohann, H. W., "High transmission polarization analyzer for Lyman-α radiation," Rev. Sci. Instrum. **58**, 359-362 (1987).
[20] Kim, J., Zukic, M., and Torr, D. G., "Multilayer thin film design as far ultraviolet polarizers," Proc. SPIE **1742**, 413-422 (1992).
[21] Bridou, F., Cuniot-Ponsard, M., Desvignes, J.-M., Gottwald, A., Kroth, U., and Richter, M., "Polarizing and non-polarizing mirrors for the hydrogen Lyman-α radiation at 121.6 nm," Appl Phys A **102**, 641–649 (2011).
[22] Kano, R., Bando, T., Narukage, N., Ishikawa, R., Tsuneta, S., Katsukawa, Y., Kubo, M., Ishikawa, S., Hara, H, Shimizu, T., Suematsu, Y., Ichimoto, K., Sakao, T., Goto, M., Kato, Yoshiaki, Imada, S., Kobayashi, K., Holloway, T, Winebarger, A., Cirtain, J., De Pontieu, Bart, Casini, R., Trujillo Bueno, J., Štěpán, J., Manso Sainz, R., Belluzzi, L., Asensio Ramos, A., Auchère, F., Carlsson, M., "Chromospheric Lyman-alpha spectro-polarimeter (CLASP)," Proc. SPIE **8443**, 84434F (2012).
[23]McIlrath, T. J., "Circular polarizer for Lyman-alpha flux," J. Opt. Soc. Am. **58**, 506-510 (1968).
[24] Gottwald F. A., Bridou, F., Cuniot-Ponsard, M., Desvignes, J.-M., Kroth, S., Kroth, U., Paustian, W., Richter, M., Schöppe, H., and Thornagel, R., "Polarization-dependent vacuum-ultraviolet reflectometry using elliptically polarized synchrotron radiation," Appl. Opt. **46**, 7797-7804 (2007).
[25] Bridou, F., Cuniot-Ponsard, M., Desvignes, J.-M., Richter, M., Kroth, U., and Gottwald, A., "Experimental determination of optical constants of $MgF_2$ and $AlF_3$ thin films in the vacuum ultra-violet wavelength region (60–124 nm), and its application to optical designs," Opt. Commun. **283**, 1351–1358 (2010).

[26] Hamm, R. N. , MacRae, R. A., and Arakawa, E. T., "Polarization Studies in the Vacuum Ultraviolet," J. Opt. Soc. Am. **55**, 1460-1463 (1965).
[27] Horton, V. G., Arakawa, E. T., Hamrn, R. N., and Williams, M. W., "A triple reflection polarizer for use in the vacuum ultraviolet," Appl. Opt. **8**, 667-670 (1969).
[28] Winter, H., Bukow, H. H., and Heckmann, P. H., "A high-transmission triple-reflection polarizer for Lyman-α radiation," Opt. Commun. **11**, 299–300 (1974).
[29] Yang, M., Cobet, C., and Esser, N., "Tunable thin film polarizer for the vacuum ultraviolet and soft x-ray spectral regions," J. Appl. Phys. **101**, 053114 (2007).
[30] Yang, M., "Design and performance of a tunable polarizer for VUV and soft x-ray spectral regions" J. Opt. A **9**, 936–939 (2007).
[31] Yang, M., Cobet, C., Werner, C., and Esser, N., "Optical polarizer integrated with suppression of higher harmonics in the vacuum ultraviolet and soft x-ray spectral regions," Appl. Phys. Lett. **92**, 011110 (2008).
[32] Smith, N. V., and Howells, M. R., "Whispering galleries for the production of circularly polarized synchrotron radiation in the XUV region," Nucl. Instrum. Meth. Phys. Res. A **347,** 115-118 (1994).
[33] Samson, J. A. R., "Polarization," chapter 9 of [Techniques of Vacuum Ultraviolet Spectroscopy], John Wiley and Sons Inc., New York (1967).
[34] Hunter, W. R., "Polarization," [Vacuum Ultraviolet Spectroscopy] *I* , J. A. Samson and D. L. Ederer, eds, Academic Press, San Diego, CA (2000).
[35] Larruquert, J. I., "Optical properties of thin film materials at short wavelengths," [Optical thin films and coatings: from materials to applications], A. Piegari, F. Flory, eds., Woodhead Publishing Series in Electronic and Optical Materials No. 49, Woodhead Publishing, Cambridge, UK (2013).
[36] Larruquert, J. I., Malvezzi, A. M., Giglia, A., Aznárez, J. A., Rodríguez-de Marcos, L., Méndez, J. A., Miotti, P., Frassetto, F., Massone, G., Nannarone, S., Crescenzio, G., Capobianco, G., Fineschi, S., "Reflective and transmissive broadband coating polarizers in a spectral range centered at 121.6 nm," J. Opt. **16**, 125713 (2014).
[37] Pasquali, L., Mukherjee, S., Terzi, F., Giglia, A., Mahne, N., Koshmak, K., Esaulov, V., Toccafondi, C., Canepa, M., Nannarone, S., "Structural and electronic properties of anisotropic ultrathin organic films from dichroic resonant soft x-ray reflectivity," Phys. Rev. B **89**, 045401 (2014).
[38] Mahne, N., Giglia, A., Sponza, L., Verna, A., Nannarone, S., "Soft-X study of buried interfaces in stratified media," Proc. SPIE **7995**, 79951S (2010).
[39] Giglia, A., Mahne, N., Bianco, A., Svetina, C., Nannarone, S., "EUV soft X-ray characterization of a FEL multilayer optics damaged by multiple shot laser beam," Nucl. Instr. Meth. A **635**, S30-S38 (2011).
[40] Jonnard, P., Le Guen, K., André, J.-M., Delaunay, R., Mahne, N., Giglia, A., Nannarone, S., Verna, A., Wang, Z.-S., Zhu, J.-T., and Zhou, S.-K., "Determination of the magnetization profile of Co/Mg periodic multilayers by magneto-optic Kerr and X-ray magnetic resonant reflectivity," J. Phys.: Conf. Ser. **417**, 012025 (2013).
[41] Tan, M. Y., Zhu, J. T., Chen, L. Y., Wang, Z. S., Le Guen, K., Jonnard, P., Giglia, A., Mahne, N., Nannarone, S., "Molybdenum-silicon aperiodic multilayer broadband polarizer for 13-30 nm wavelength range," Nucl. Instr. Meth. A **654**, 588-591 (2011).
[42] http://www.elettra.trieste.it/it/lightsources/elettra/elettra-beamlines/bear/bear.html
[43] Schäfers, F., Mertins, H.-C., Gaupp, A., Gudat, W., Mertin, M., Packe, I., Schmolla, F., Di Fonzo, S., Soullié, G., Jark, W., Walker, R., Le Cann, X., Nyholm, R., and Eriksson., M., "Soft-x-ray polarimeter with multilayer optics: complete analysis of the polarization state of light," Appl. Opt. **38**, 4074-4088 (1999).
[44] Larruquert, J. I., Aznárez, J. A., Rodríguez-de Marcos, L., Méndez, J. A., Malvezzi, A. M., Giglia, A., Miotti, P., Frassetto, F., Massone, G., Nannarone, S., Crescenzio, G., Capobianco, G., Fineschi, S., "Multilayer reflective polarizers for the far ultraviolet," Proc. SPIE **8777**, 87771D (2013).
[45] Hofmann, A., [The Physics of Synchrotron Radiation], Chapter 5, Cambridge University Press, Cambridge, UK, (2004).
[46] Fineschi, S., Gardner, L. D., Kohl, J. L., Romoli, M., Pace, E., Corti, G., Noci, G., "Polarimetry of the UV Solar Corona with ASCE," Proc. SPIE **3764**, 147-160 (1999).